HYDRONAUTICS, Incorporated

TECHNICAL REPORT 121-5

THE SHAPE OF CAVITIES IN SUPERCAVITATING FLOWS

By

Marshall P. Tulin

April 1965

Presented in Abridged Form at the XI International Congress
for Theoretical and Applied Mechanics, Munich -
September 1964

Prepared Under

Contract Nonr-3435(00)
Office of Naval Research
Navy Department

TABLE OF CONTENTS

NOTATION

A, b_r, b_i, c_i	Real constants
C_D	The drag coefficient based on a characteristic body dimension, c
C_d	The drag coefficient based on the cavity length, ℓ
c	A characteristic body dimension
c_p	The pressure coefficient on the body
g	The acceleration of gravity
I	Denotes "the imaginary part of"
k	A wave number, $g\ell/2U_o^2$
ℓ	A non-dimensional length, $g\ell/2U_o^2$
ℓ_o	The cavity length in the absence of gravity
p_∞	The ambient pressure at the position of the forebody
p_c	The pressure in the cavity
R	Denotes "the real part of"
$t(\infty)$	The wake or cavity thickness at infinity
t_c	The cavity thickness
U_c	The speed on the cavity

U_o	The speed at infinity
u	The velocity perturbation in the undisturbed flow direction
v	The velocity perturbation normal to u
$\forall$	The total volume of the cavity
x	The ordinate in the undisturbed flow direction
y	The ordinate normal to x
y_c	The vertical ordinate of the cavity boundary
y_o	The vertical ordinate of the body
z	The complex variable, x + iy
$\alpha_o, \alpha_1, \alpha_2, \beta, \gamma$	Real constants
Γ	The circulation around the cavity
ζ	The non-dimensional complex variable, $\frac{x + iy}{\ell/2}$
ν	The complex velocity, u - iv
ξ	The non-dimensional horizontal ordinate, $\frac{x}{\ell/2}$
ρ	The density of the flowing fluid
σ	The cavitation number based on the ambient pressure at the forebody, $\sigma = \frac{p_\infty - p_c}{\frac{1}{2}\rho U_o^2}$
τ	The entering incidence

Φ	The complex potential, $\phi + i\psi$
$\tilde{\Phi}$	The non-dimensional complex potential, $\frac{\Phi}{U_o \cdot \ell/2}$
ϕ	The real velocity potential
ψ	The real stream function
$\tilde{\psi}$	The non-dimensional stream function, $\frac{\psi}{U_o \cdot \ell/2}$

INTRODUCTION

A great deal of interest has recently been shown in supercavitating flows. This interest seems due in part to the subject's practical importance in connection with supercavitating and ventilated propellers, turbines, and hydrofoils; in part to the traditional mathematical interest in free streamline flows — as boundary value problems; and perhaps in part to the stimulation afforded by the observation of actual supercavitating flows as created in experimental water channels. Indeed, "cavity-watching" can be a rewarding past-time, and no better way to become familiar with cavity flows can be imagined. Sometimes interesting phenomena which are not yet well understood may be observed, and occasionally one is moved to ask quite general questions about the shape of cavities in supercavitating flows. The latter forms the subject of this paper.

Some of the most interesting cavities in nature are unsteady and three-dimensional. Here, however, we shall discuss only certain questions about steady, planar flows.

Perhaps the most interesting new result given here concerns the effect of a transverse gravity field on the Helmholtz flow ($\sigma = 0$) past a small forebody experiencing drag alone. The first-order boundary value problem for this flow is solved in closed form. It is shown that the cavity behind such a body is of a finite length which corresponds to a definite Froude number [flow speed/$(g \times \text{cavity length})^{\frac{1}{2}}$] with a value of $1/\sqrt{\pi}$. The cavity is, quite contrary to intuition, deflected in the same direction in which gravity acts, so that the bulk of the cavity lies below the forebody; the cavity is symmetric fore and aft and terminates at the depth of the forebody.

Other flows are also discussed here including the dragless cavity, and some new non-linear finite-cavity models are discussed; these models feature cavity termination in spiral vortices followed by trailing wakes.

STEADY, PLANAR CAVITIES IN THE ABSENCE OF GRAVITY

The length of a cavity which is at least several times in length the size of the body that produces it, depends primarily on the drag of the forebody (which is assumed to be non-zero) and the cavitation number of the flow. The form of the well-known asymptotic law,

$$\ell/c \sim C_D \sigma^{-2} \qquad [1]$$

may be deduced from some rather simple considerations, Tulin (1964), of which the most important is that the cavity drag of the forebody manifests itself in the flow in the form of mixing momentum losses; these are assumed to occur in a localized region where the cavity terminates or "collapses." Irregular, turbulent flow has often been observed in this region, Figure 1a.

In the special and historically very important case of the Helmholtz flow ($\sigma = 0$ and gravity, surface tension, etc. are absent) the cavity becomes infinite in extent. The drag of the forebody then manifests itself in a convection of momentum aft. If the possibility of asymptotic waves on the cavity is ignored, then it may easily be deduced from momentum consideration that the drag of the forebody is finite but non-zero only if the cavity width increases asymptotically as the square root of the downstream distance; in fact, it is necessary that

$$y_c/c \sim \left(\frac{2}{\pi} C_D\right)^{\frac{1}{2}} (x/c)^{\frac{1}{2}} \qquad [2]$$

This is indeed the correct asymptotic behaviour in this case, for waves certainly cannot occur on the cavity without the presence of gravity, surface tension, a basic shear flow, or some other agency which might cancel the inevitable undulations in dynamic pressure which must occur along the wavy free streamline.

It is clear that the presence of gravity, regardless of its strength, must cause a complete alteration of the asymptotic field as given by [2], for a cavity of unbounded width cannot exist at constant pressure in the presence of even the slightest transverse gravity field. Later on we shall quantitatively describe the very interesting effect of gravity, but for now we continue to ignore it.

The shape of finite cavities ($\sigma > 0$) cannot be defined through ideal flow considerations alone, for a steady finite cavity at constant pressure cannot exist in a perfect fluid. Observations indicate, however, that unsteady and viscous effects are important in the cavity flow, only in the immediate region of cavity collapse, and in the wake of the cavity which trails downstream. Starting with Zhukovsky (1890) various assumptions about the flow behind the cavity and/or at closure have been made in the form of mathematical models which allow solutions. These are perhaps best evaluated with regard to their relevancy by considering briefly the real cavity flow.

A viscous wake, trailing to infinity downstream, must exist behind a real finite cavity in nature, Figure 1b. Momentum considerations require that the forebody drag experienced by a real supercavitating body be manifested by a momentum defect in the far wake behind the body and its cavity. Cavity drag must therefore manifest itself in much the same way as friction and form drag do in the flow past a body without a cavity. In this latter case, it is a matter of experience that the displacement thickness of the wake generally decreases continuously from the region right behind the body, toward an asymptotic value equal to the momentum thickness; this behaviour is due to the continual downstream smoothing of the blunt wake profile found close to the body itself. We should expect precisely the same behaviour of the cavity-wake displacement thickness since the wake profile must be most blunt in the turbulent region just behind cavity collapse — the region where the momentum losses are actually experienced by the fluid. The effect of the wake on the outer potential flow may be determined by replacing it with a body whose thickness is taken equal to the wake displacement thickness. The asymptotic thickness of the trailing wake is thus,

$$\frac{t(\infty)}{c} \sim \frac{C_D}{2} \qquad [3]$$

For blunt bodies, whose drag coefficient is O(1), the wake thickness according to [3] is about the same size as the body itself, and should <u>not</u> therefore be neglected in any proper model of the flow. At the same time, the wake thickness is seen to be somewhat <u>thinner</u> than the body width for $C_D < 2$, as is always the case for small and moderate value of $\sigma (\sigma < 1)$; therefore, a proper model must neither ignore the wake nor involve too wide a trailing wake.

For slender bodies, whose drag coefficient is of the order of the body thickness or inclination squared, the wake thickness according to [3] need only arise in connection with second-order terms; that is, a linearized or first order theory may properly neglect the wake.

All well-known wake models may be divided into two categories. They either involve no trailing wakes at all: Riabouchinsky (1920); Efros (1946) - Kreisel (1946) - Gilbarg (1946); and Tulin (1953); or they involve thick wakes whose thickness is generally greater than that of the frontal projection of the body:

Zhukovsky (1890) - Roshko (1955) - Eppler (1954), and Wu (1962) - Fabula (1962). The former of these groups is clearly more suitable for the treatment of slender bodies, and the latter for blunt bodies. Note, however, that even in the case of blunt bodies, the latter group of models will generally very much exaggerate the wake thickness. In any case, none of the models mentioned is suitable for the proper representation of supercavitating flow past both blunt and slender bodies.

In Figure 2 are presented two cavity flow models involving cavities which terminate in spiral vortices and are followed by trailing wakes. These flows resemble in a number of important respects our description of real cavity flows. Their asymptotic wake thicknesses are adjusted always, to be in proper relation to the drag coefficient. In the case of the double spiral vortex model, the trailing wake thins downstream, imitating the downstream reduction in the displacement thickness of a real wake. The double spiral vortex model further attempts to reflect reality roughly by taking into account the loss in pressure recovery which must surely accompany mixing at cavity collapse; it does this by assuming that ambient, rather than stagnation pressure exists in the wake just behind the region of cavity collapse as well as far downstream. These models, in the particular case where the wake is closed at infinity, were first suggested by Tulin (1964), in connection with a discussion of small perturbation theory. As noted then, the use of either spiral vortex model may also afford satisfaction through their representation of the turbulent mixing at cavity collapse by the physically impossible (the physical plane is infinitely covered in their neighborhood) but nevertheless highly suggestive spiral vortices.

Mathematically, these spiral vortex models offer important advantages. The single vortex termination involves a wake which is closed in the physical plane to the first order, which is continuous across $\psi = 0$ in the ϕ, ψ plane, and which affords a particularly good model from which to proceed with a small perturbation expansion; the reason for the latter lies in the fact that the boundary value problem for the second order expansion for this model is with the exception of the wake closure condition, identical in form with the first order problem, while the latter is identical with that which provides the usual starting point for the linearized theory, Tulin (1964). The double spiral vortex model corresponds to a flow in a simply connected region in the ϕ, ψ plane. This affords a very considerable advantage when treating the problem of a foil beneath a free surface at high speeds, and has just recently been used in a first order theory to treat that problem with very good agreement between theory and experiment, Yim (1964).

Linearized, or first order theory, may be used to produce quite general results about cavity shapes in supercavitating flows. When the trailing wake is thin or non-existent, the cavity behind a body approaches an elliptic shape, whose thickness ratio is just $\sigma/2$, Tulin (1953). In this first order theory the region of cavity collapse shrinks down to a point singularity. If the cavity length is ℓ, then the complex velocity near cavity termination takes the form:

$$\nu \sim (z - \ell)^{-\frac{1}{2}} \left(\frac{\text{Drag}}{\frac{1}{2}\rho U_c^{2} . 2\pi} \right)^{\frac{1}{2}} \qquad [4]$$

If the cavity is much longer than the forebody, then the latter may sometimes be represented by a similar singularity placed at the leading edge of the cavity; such a "point body" can be very useful, and has been used to derive many of the results presented below.

The first order solution corresponding to the single spiral vortex model and to a point body is:

$$\nu = -\frac{\sigma}{2} \frac{(z-\beta\ell)}{[z(z-\ell)]^{\frac{1}{2}}} + \frac{\sigma}{2} \qquad [5]$$

where

$$\beta\ell = \frac{\sqrt{\ell}}{\sigma} \left(\frac{2 \text{ Drag}}{\pi . \frac{1}{2}\rho U_c^{2}} \right)^{\frac{1}{2}}$$

If wake closure at infinity is assumed, then this solution requires that:

$$\ell/c = \frac{8}{\pi} \frac{C_D}{\sigma^2} \quad \text{or} \quad \beta = 1/2 \qquad [6]$$

This is the result of the usual linearized theory, Tulin (1955).

If, however, a non-zero asymptotic wake is allowed according to [3], then $\beta > 1/2$ and:

$$\ell/c = \frac{8}{\pi} \frac{C_D}{\sigma^2} \left[\frac{1 + \sqrt{1-\sigma/4}}{2} \right]^2 \qquad [7]$$

so that the cavity is shortened due to the thickness of the trailing wake. The first order wake is of constant thickness from cavity termination to far downstream.

The model with constant pressure wake (double spiral vortex) produces quite a different first order solution for the flow past a point body. For a closed wake at infinity,

$$\nu = - \frac{i\sigma}{\pi} \left[\sqrt{\frac{\ell}{z}} + \frac{1}{2} \ln \left(\frac{\sqrt{z} - \sqrt{\ell}}{\sqrt{z} + \sqrt{\ell}} \right) \right] \qquad [8]$$

The length of the cavity is:

$$\ell/c = \frac{\pi}{2}\frac{C_D}{\sigma^2} \qquad [9]$$

so that the cavity is shorter in the ratio $\pi^2/16$ than with the usual closed cavity model, [5]. The cavity is now no longer elliptic in shape, and it has of course, a non-zero thickness at cavity termination.

Regarding the relative validity of these models there is some evidence that [9] is closest to reality, but more experimentation is needed to finally decide upon the relevancy of these and other proper cavity models. Such experiments must carefully take heed of the important influence on cavity length of walls, free surfaces, three-dimensional effects, gravity, etc.

Dragless Cavities

Not all supercavitating bodies possess drag. In the design of ventilated struts for high speed hydrofoil craft it is very important to minimize their cavity drag, and it has been shown how this may be done, even in some cases to the extent that the drag vanishes, Tulin (1962), Johnson and Starley (1962). In that case, however, the questions arise: what is the law for the cavity length, replacing [6], [7] or [9] and what is the flow like in the region of cavity termination?

These questions are readily answered for slender bodies and for long cavities, which allow us to consider again a point forebody (placed at $z = 0$). The singularity representing this forebody must, however, be of higher order than in [5] or [8], since it produces no drag. If the cavity is of length ℓ, then we may show that the pertinent first order solution is:

$$\nu = \frac{(z-\ell)^{\frac{1}{2}}}{z^{3/2}} \left[\gamma - \frac{\sigma}{2} \cdot z\right] + \sigma/2 \qquad [10]$$

where

$$\gamma^2 = \frac{1}{4\pi\ell} \int_{\text{forebody}} c_p \cdot \frac{dy_o}{dz} \cdot z^2 dz \qquad [11]$$

In this expression, c_p is the pressure coefficient, so that the integral represents a second moment of the drag. There should exist no wake behind a dragless cavity, so that the cavity should be closed. Then $\lim_{z \to \infty} \nu \sim 1/z^2$, which requires that:

$$\ell/c = (4/\pi)^{1/3} \frac{\gamma^{2/3}}{c} \cdot \sigma^{-2/3} \qquad [12]$$

This is the law for the cavity length of supercavitating bodies with no drag; as might be expected, the length of these cavities increases much less rapidly with decreasing cavitation number than those produced by bodies with drag.

The shape of the dragless cavity is cusped at its trailing edge, i. e. $y_c \sim (z-\ell)^{3/2}$.

The Influence of Lift

The meanline of the cavity is warped by lift in the direction opposite to that in which the lift acts. The deflection of the cavity approaches $\ln x$ and is thus unbounded in the case of the Helmholtz flow ($\sigma = 0$). This warping is the main effect due to lift (gravity absent); the thickness distribution remains relatively undisturbed. According to first order theory, Tulin (1955), the asymptotic cavity length depends only on the body drag, while the cavity thickness distribution only depends upon the thickness of the forebody; and neither depends upon the incidence or lift of the body — except insofar as these change the forebody shape or drag.

STEADY, PLANAR CAVITIES IN THE PRESENCE OF GRAVITY

Gravity can exert an extraordinary influence on the shape and length of cavities in supercavitating flow. The actual magnitude of its effect depends upon a Froude number ($U_o/\sqrt{g\ell}$), and upon the orientation of the gravity field relative to the flow direction.

Longitudinal Field

A gravity field co-incident with the flow direction (longitudinal field) which acts upon a cavity created by a point drag forebody does not disturb the vertical symmetry of the flow, but does alter the shape and length of the cavity. We shall see that regardless of the sign or magnitude of g, its effect is to prevent the existence of cavities of infinite length ($\sigma \geq 0$).

In the case of a field pointing in the same direction as the flow the cavity is shortened; if the cavitation number is taken as based on the pressure immediately at the forebody, then clearly the cavity length is finite even in the case where $\sigma = 0$. The cavity becomes squashed-elliptic in shape; the after part being more blunt than the forward part.

When the field points in a direction opposed to that of the flow, the cavity is lengthened and its after part becomes less blunt than its forward part. Finally, the field strength having increased to a critical value, the trailing edge of the cavity becomes cusped, rather than blunt. For stronger fields, no steady cavity flow seems to exist. All of these effects were pointed out in earlier studies of the problem by Acosta (1961) and Lenau (1963).

The squashing effect of the gravity field upon the cavity is not difficult to explain. The total drag of the body plus cavity due to dynamic pressures (i.e. excluding gravity) must be null, as the body plus cavity is closed. At the same time, the actual pressure on the cavity is constant except at the singular point which represents cavity collapse. As a consequence, the buoyancy force on the cavity must be precisely equal to the difference between the drag of the body and the upstream force which would act on the cavity at its very end if it were a solid body. For a gravity field in the direction of flow, the buoyancy acts upstream; therefore the upstream force must be larger than the body drag. This requires that the cavity be more blunt at its downstream end. The opposite is true when gravity points upstream, and in this case, the cavity becomes cusped (no upstream force) when the forebody drag is precisely equal to the buoyancy force acting upon the cavity. For stronger fields this buoyancy force cannot be balanced, and so no steady solutions exist.

The first order solution for the point drag forebody and for the usual closed cavity model is:

$$\nu = \frac{(\ell g/4U_o^2) - \zeta[(\ell g/2U_o^2) + \sigma_o/2] - \zeta^2(\ell g/2U_o^2)}{(\zeta^2 - 1)^{\frac{1}{2}}} + \frac{\sigma_o}{2} + (\zeta + 1)\ell g/2U_o^2 \qquad [13]$$

where,

$$\ell/c = \frac{8}{\pi\sigma^2} \frac{C_D}{\left[1 + \frac{\ell g}{2U_o^2\sigma}\right]^2} \qquad [14]$$

In the case of positive g fields (acting downstream), the maximum cavity length, which occurs when $\sigma = 0$, is

$$(\ell/c)_{max} = \left(\frac{8}{\pi}\right)^{1/3} \frac{(C_D)^{1/3}}{(gc/2U_o^2)^{2/3}} \quad (g > 0) \qquad [15]$$

while the maximum length, corresponding to the cusped cavity condition, for negative g fields is,

$$(\ell/c)_{max} = \left(\frac{8}{\pi}\right)^{1/3} \frac{(C_D)^{1/3}}{(gc/U_o^2)^{2/3}} \quad (g < 0) \qquad [16]$$

and this occurs when,

$$\sigma = -\frac{3}{2}\frac{g\ell}{U_o^2} \qquad [17]$$

It is useful to note that the cavity length according to [14] corresponds in the general case precisely to that for a cavity-free field, [5], providing that the cavitation number for the flow is based not in the usual way on the ambient pressure at the forebody itself, but rather on the ambient pressure at a distance $\ell/4$ downstream of the forebody.

The case of the longitudinal gravity field produces interesting results, but it should be appreciated that it involves a somewhat artificial situation. A body actually moving vertically through the ocean would have to adjust its cavity pressure continuously in order to maintain a constant cavitation number at the forebody, and in addition the speed of the body would in the general case itself be varying. Thus real cavity flows involving longitudinal gravity fields are in most cases unsteady and the effects of unsteadiness can easily predominate. Of course, steady fields of this kind can be created in water tunnels with vertical sections and, artificially, through interference fields due to neighboring bodies.

Transverse Gravity Fields

A more natural situation involves a horizontal supercavitating flow in the presence of a vertical or transverse gravity field. This flow has received some attention, Parkin (1957), Street (1963), and Ivanov (1961), but in each case at the expense of rather broad assumptions which restrict the applicability of the results. Typically the assumption has been made that the ambient pressure is constant on each of the free streamlines, being lower than the reference pressure at the forebody on the upper, and higher than this reference pressure on the lower streamline. These "average" ambient pressures are determined as the average head of each streamline as it passes between the forebody and the point of cavity collapse. The rather basic question regarding the form of the steady two-dimensional cavity in the case of zero cavitation number (that is, the Helmholtz flow with transverse gravity) has been completely untouched. An answer to this question based on first order considerations and the usual closed cavity model is given here; an exact solution of the first order problem is obtained. It would seem clear that this answer to the question of transverse gravity effects is not a mere product of the perturbation approximations, but applies, in general, to the non-linear situation, assuming that either the re-entrant jet, single spiral vortex, or Riabouchinsky models are used. The first order solution given here includes, not only the case $\sigma = 0$, but the general case $\sigma > 0$.

We begin by phrasing the first order boundary value problem, assuming a cavity of unknown length, ℓ, created by a point drag. The pressure is constant, p_c, on the cavity everywhere except at the point forebody and at the point of cavity collapse, $z = \pm\ \ell/2$. Taking into account a gravity field directed downward, Bernoulli's equation becomes to the first order,

$$\frac{p_\infty - p_c}{\frac{1}{2}\rho U_o^{\,2}} = \sigma = 2\left(\frac{u}{U_o} + \frac{gy_c}{U_o^{\,2}}\right) \quad \text{on the cavity} \qquad [18]$$

or,

$$\frac{p_\infty - p_c}{\frac{1}{2}\rho U_o^2} = \sigma = 2\left(\frac{u}{U_o} - \frac{g\psi}{U_o^3}\right) \quad \text{on the cavity} \qquad [19]$$

where use has been made of the relation,

$$y_c(x) = \int_{-\ell/2}^{x} v/U_o \, dx = -\frac{1}{U_o}[\psi(x) - \psi(-\ell/2)] \qquad [20]$$

and where $\psi(-\ell/2)$ is taken to be zero.

Equation [19] may be written in terms of the complex potential,

$$R\left[\Phi' + i\frac{g}{U_o^2}\Phi\right] = \frac{\sigma U_o}{2} \quad \text{on the cavity} \qquad [21]$$

or, in non-dimensional form,

$$R[\tilde{\Phi}' + ik\tilde{\Phi}] = \sigma/2 \qquad \text{on the cavity} \qquad [22]$$

where R denotes "real part of"; $k = \frac{g\ell}{2U_o^2}$; $\tilde{\Phi}(\zeta) = \frac{\phi + i\psi}{\ell/2 \cdot U_o}$; and $\zeta = \frac{z}{\ell/2}$.

Since the pressure is constant on the cavity everywhere except at $z = \pm\ \ell/2$, and since the net drag on the body must be null, a "counter-force" must exist at $z = +\ \ell/2$ just equal in magnitude to the forebody drag (of course, this force does not really act on the cavity, but rather represents momentum loss in the flow). Therefore,

$$\lim_{\zeta \to \pm 1} [(\zeta \mp 1)^{\frac{1}{2}} \cdot \tilde{\Phi}']^2 = \frac{C_d}{2\pi} \qquad [23]$$

where

$$C_d = \frac{\text{Drag}}{\frac{1}{2}\rho U_o^2 \cdot \ell/2}$$

Further the cavity is closed. Therefore,

$$I \cdot \oint \tilde{\Phi}'\, d\zeta = 0 \qquad [24]$$

where I denotes imaginary part of and the contour integral is taken completely around the body and cavity.

The asymptotic nature of the solution may be deduced in advance. The closed cavity plus body must possess no net lift since the pressure or the cavity is constant and the forces at the ends are purely longitudinal (the body has drag, but no lift). Therefore a dynamic lift equal and opposite to the net vertical buoyancy must exist on the body. As a result the asymptotic expansion of the velocity field must have the following form,

$$\tilde{\Phi}' \sim i\left(\frac{L}{\pi\rho U_o^{\,2}\ell}\right)\frac{1}{\zeta} + \left(\frac{2L}{\pi\rho g\ell^2}\right)\frac{1}{\zeta^2} + \frac{ib_i}{\zeta^2} + 0\left(\frac{1}{\zeta^3}\right) \qquad [25]$$

where L is the dynamic lift. The coefficient b_i is real and is associated with the longitudinal asymmetry of the cavity (it happens to vanish in the present case).

The analytic function $[\tilde{\Phi}'' + ik\,\tilde{\Phi}']$ must exhibit the following characteristics, according to [22], [23], and [25]:

$$R\,.\,[\tilde{\Phi}'' + ik\,\tilde{\Phi}'] = 0 \quad \text{on the cavity} \qquad [26]$$

$$[\tilde{\Phi}'' + ik\,\tilde{\Phi}'] \sim -\left(\frac{kL}{\pi\rho U_o{}^2 \ell}\right) \cdot \frac{1}{\zeta} \quad \text{for large } \zeta \qquad [27]$$

$$\lim_{\zeta \to \pm 1} [\tilde{\Phi}'' + ik\,\tilde{\Phi}'] \sim \frac{\sqrt{C_d/\pi}}{(\zeta^2 - 1)^{3/2}} \qquad [28]$$

These requirements are met by the function,

$$\tilde{\Phi}'' + ik\,\tilde{\Phi}' = \frac{\alpha_o + \alpha_1\zeta + \alpha_2\zeta^2}{[\zeta^2 - 1]^{3/2}} \qquad [29]$$

where,

$$\alpha_1 = 0 \qquad [30]$$

$$\alpha_2 = \left(\frac{-kL}{\pi\rho U_o{}^2 \ell}\right) \qquad [31]$$

$$\alpha_o + \alpha_2 = \sqrt{\frac{C_d}{\pi}} \qquad [32]$$

It may be shown by inspection of the asymptotic field that the asymmetry about $\xi = 0$ of the vorticity represented by [29] is proportional to α_1; in the present case, then, this vorticity is symmetric. There are a number of important consequences: the camber line of the cavity must be symmetric fore and aft, so that the cavity terminates at the depth of the forebody; and the cavity thickness must be symmetric fore and aft.

The cavity shape may be found from the following relationships,

$$I \,.\, [\tilde{\Phi}'' + ik\,\tilde{\Phi}'] = \frac{d^2\tilde{y}_c}{d\xi^2} + k^2\tilde{y}_c - \frac{\sigma}{2}\,k \qquad [33]$$

or,

$$\frac{d^2\tilde{t}_c}{d\xi^2} + k^2\tilde{t}_c = \frac{-2(\alpha_o + \alpha_2\xi^2)}{(1 - \xi^2)^{3/2}} \qquad [34]$$

and,

$$\frac{d^2\tilde{y}_m}{d\xi^2} + k^2\tilde{y}_m = +\,\frac{\sigma k}{2} \qquad [35]$$

These differential equations for the cavity thickness (t_c) and camber (y_m) may be solved, making use of available conditions.

$$\tilde{t}_c = -2\int_{-1}^{\xi} \cos k(\xi-\xi')\left[\frac{(\alpha_o+\alpha_2)\xi'}{\sqrt{1-\xi'^2}} + \alpha_2 \cos^{-1}\xi' - \pi\alpha_2\right] d\xi' \quad [36]$$

where the last term $(-\pi\alpha_2)$ within the brackets has been chosen in order to make $\tilde{t}_c$ symmetric about $\xi = 0$. An alternative expression which is more suitable for numerical computation is,

$$\tilde{t}_c = -2(\alpha_o+\alpha_2)\left[\cos k\xi\int_{-1}^{\xi} \frac{\xi'\cos k\xi' d\xi'}{(1-\xi'^2)^{\frac{1}{2}}} + \sin k\xi\int_{-1}^{\xi} \frac{\xi'\sin k\xi' d\xi'}{(1-\xi'^2)^{\frac{1}{2}}}\right]$$

$$+ \frac{2\alpha_2}{k}\left[\sin k\xi\int_{-1}^{\xi} \frac{\cos k\xi' d\xi'}{(1-\xi'^2)^{\frac{1}{2}}} - \cos k\xi\int_{-1}^{\xi} \frac{\sin k\xi' d\xi'}{(1-\xi'^2)^{\frac{1}{2}}}\right] \quad [37]$$

The cavity must be closed, $t_c(+1) = 0$, so that,

$$(\alpha_o + \alpha_2)\int_{-1}^{+1} \frac{\xi' \sin k\xi' d\xi'}{\sqrt{1-\xi'^2}} = \frac{(\alpha_2)}{k}\int_{-1}^{+1} \frac{\cos k\xi' d\xi'}{\sqrt{1-\xi'^2}} \tag{38}$$

or,

$$\frac{\alpha_2}{(\alpha_o + \alpha_2)} = \frac{kJ_1(k)}{J_o(k)} \tag{39}$$

The camber, again symmetric fore and aft, is the integral of [35]:

$$\tilde{y}_m = - \frac{\sigma}{2k \cos k} (\cos k\xi - \cos k) \tag{40}$$

This camber generates a dynamic lift which may be calculated according to thin airfoil theory, with the result,

$$\frac{L}{\rho U^2 \ell/2} = - \frac{\sigma\pi}{\cos k} \cdot J_1(k) \tag{41}$$

so that in view of [31],

$$\alpha_2 = \frac{\sigma k J_1(k)}{2 \cos k} \qquad [42]$$

and, combining [39], [42], and [32], a relation between wave number, drag coefficient, and cavitation number is finally obtained,

$$\frac{2}{\sigma}\sqrt{\frac{C_D}{\pi}} = \frac{\cos k}{J_o(k)} \qquad [43]$$

In the case k = 0 (no gravity), it follows from [43] that,

$$\ell_o = \frac{8}{\pi}\,\frac{\text{Drag}}{\rho U_o{}^2/2} \cdot \frac{1}{\sigma^2} \qquad [44]$$

which is the correct result for this model.

When $k \neq 0$, we may derive from [43] the result,

$$\ell/\ell_o = \frac{\cos^2 k}{J_o{}^2(k)} \qquad [45]$$

where ℓ_o is the length when k = 0, [44].

In the special case of the Helmholtz flow ($\ell_o = \infty$), the cavity length corresponds to a particular value of k, which is independent of the drag. It is given by $\cos^2 k = 0$, or

$$k = \frac{g\ell}{2U_o^2} = \frac{\pi}{2} \qquad [46]$$

This is a central result of this analysis, for it reveals that a transverse gravity field causes the cavity length to be finite even in the case $\sigma = 0$, and that the resulting cavity length corresponds to a definite Froude number,

$$\frac{U_o}{\sqrt{g\ell}} = \frac{1}{\sqrt{\pi}} \quad . \qquad [47]$$

The cavity shape has been calculated on a digital computer, using [38] and [40], and the result is shown in Figure 3. The camber line is deflected downward but has positive curvature (negative camber). The cavity is symmetric about its midpoint.

Clearly, the effect of transverse gravity on the cavity length will be extraordinary for suitably small σ. The importance of gravity in the general case is revealed by computations based on [45]. The result is shown in the Table below, where ℓ_o is given by [44].

TABLE 1

The Effect of Transverse Gravity on Cavity Length

	($\sigma = 0$) ↓											($g = 0$) ↓
ℓ/ℓ_o	0	.02	.05	.09	.19	.29	.39	.50	.71	.82	.97	1.0
$\frac{g\ell_o}{2U_o^2}$	∞	80	29	16	7	4	2.8	2.0	1.1	.73	.31	0

It appears that in order to reduce the effect of transverse gravity on the cavity length to the extent that $\ell/\ell_o > .97$, a Froude number based on cavity length, $\frac{U_o}{\sqrt{g\ell}}$, in excess of about 1.25 is required.

A further effect of gravity is to cause the flow just in front of the forebody to enter with a negative incidence, as was deduced earlier by Ivanov (1961); this may be seen from the negative slope of the cavity camber line at the forebody, Figure 3. The entering incidence τ for $\sigma = 0$ is:

$$\tau = - \frac{1}{J_o(\pi/2)} \cdot \sqrt{\frac{C_d}{\pi}} = - .95 \left[C_D \cdot \frac{gc}{U_o^2}\right]^{\frac{1}{2}} \qquad [43]$$

This incidence, which tends to produce a negative lift on the forebody, may take on significant values. Take, for example, $C_D = .03$, $c = 5$ ft., and $U_o = 70$ ft. sec.; then $\tau \approx -1.5^{\circ}$.

Forebody lift will clearly have a marked effect on cavity shape in the presence of transverse gravity — in contrast to the case where gravity is absent. This effect will be due in the first place to the warping effect of the lift on the cavity camber line, which results in alterations of the local cavitation numbers. It seems clear that positive lift, which deflects the cavity downward, will result in further shortening of the cavity, while negative lift should cause its length to increase. The entering incidence due to gravity warping will as a result be altered. In addition, the effect of gravity on cavities of finite span may be quite different than we have revealed here for two-dimensional cavities. In fact, it seems most probable that cavities of very low aspect ratio (as shed from bodies of revolution, for instance) will <u>not</u> be deflected downwards by a downward pointing gravity field but will, on the contrary, float upwards.

These and many other interesting and important problems regarding the shape of cavities in supercavitating flows yet remain to be explored.

REFERENCES

ACOSTA, A. J. 1961 - Jour. Appl. Mech. Vol. 28, Ser. E, No. 2.

EFROS, D. A. 1946 - Doklady Akad. Nauk, CCCR, Vol. 51, No. 4.

EPPLER, R. 1954 - Jour. Rat. Mech. Analy., Vol 3.

FABULA, A. 1962 - Jour. Fluid Mech., Vol. 12, Part 2.

GILBARG, D. and ROCK, D. 1946 - Naval Ord. Lab. Memo 8718.

IVANOV, A. I. 1961 - Sudostroeniye (CCCR), No. 2.

JOHNSON, V. E., and STARLEY, S. E. 1962 - Proc. Inst. Aero. Sci. Symp. Hydrofoils.

KREISEL, G. 1946 - Admiralty Res. Lab. Rpt. No. R1/H/36.

LENAU, C. W. 1963 - Stanford Univ. Civil Engr. Dept. Tech. Rpt. No. 28.

PARKIN, B. R. 1957 - Calif. Inst. Tech. Engr. Div. Rpt. No. 47-9.

RIABOUCHINSKY, D. 1920 - Proc. London Math. Soc., Vol. 19, Ser. 2.

ROSHKO, A. 1955 - Jour. Aero. Sci., Vol. 22, No. 2.

STREET, R. L. 1963 - Jour. Ship. Res. Vol 7, No. 1.

TULIN, M. P. 1953 - David Taylor Model Basin Rpt. 834.

TULIN, M. P. 1955 - Proc. N.P.L. Symp. Cavit. Hydrodynamics, Philosophical Library.

TULIN, M. P. 1962 - Proc. General Motors Symp. Cavit. Real Fluids, Elsevier Press.

TULIN, M. P. 1964 - Jour. Ship. Res., Vol. 3, No. 3.

WU, T. Y. 1962 - Jour. Fluid Mech., Vol. 13, Part 2.

YIM, B. 1964 - HYDRONAUTICS, Incorporated Tech. Rpt. 463-4.

ZHUKOVSKY, N. E. 1890 - Matematicheskii Sbornik (CCCR), Vol. XV.

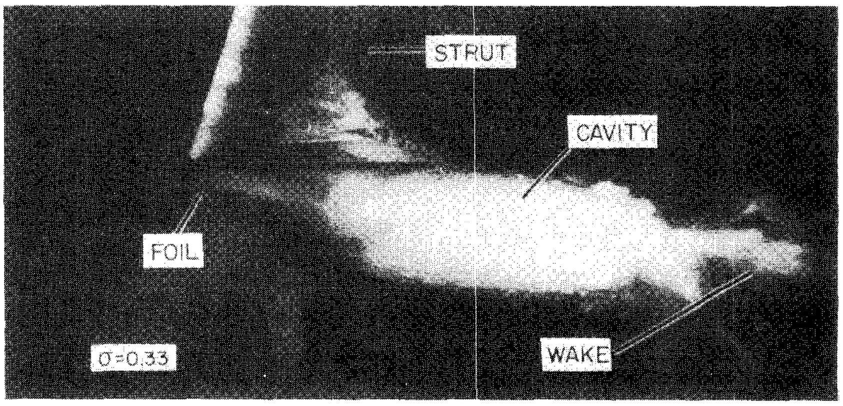

FIGURE 1(a)-PHOTOGRAPH OF CAVITY CALLAPSE AND WAKE

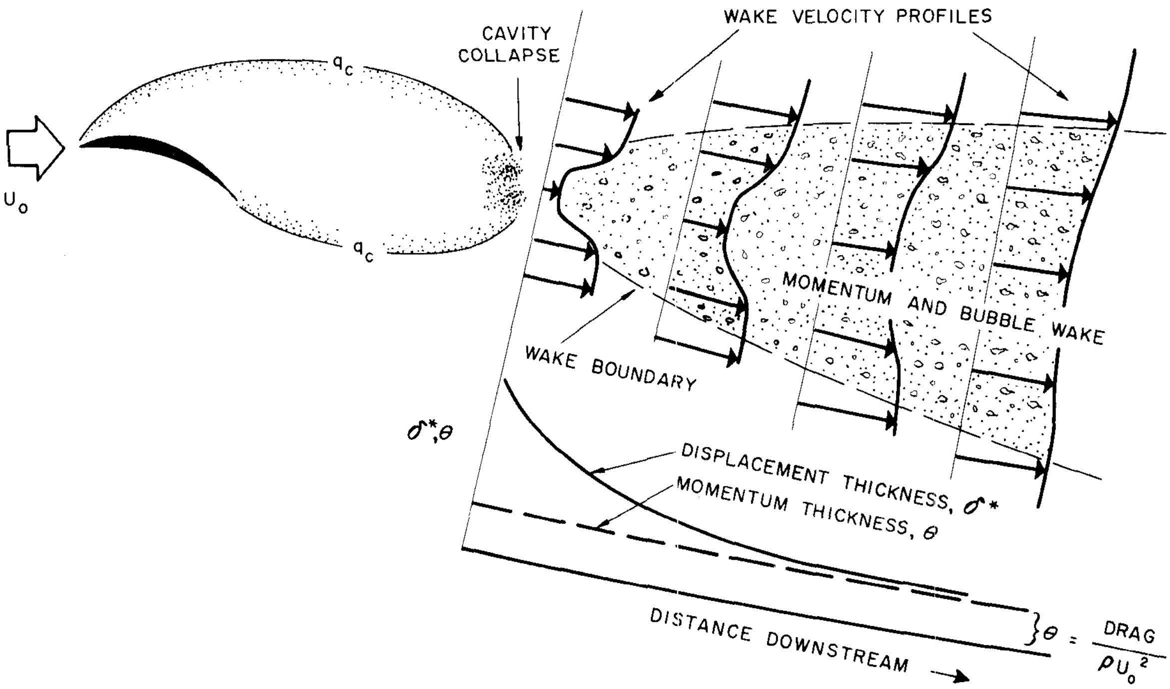

FIGURE 1(b)-SCHEMATIC OF A WAKE REAL CAVITY FLOW

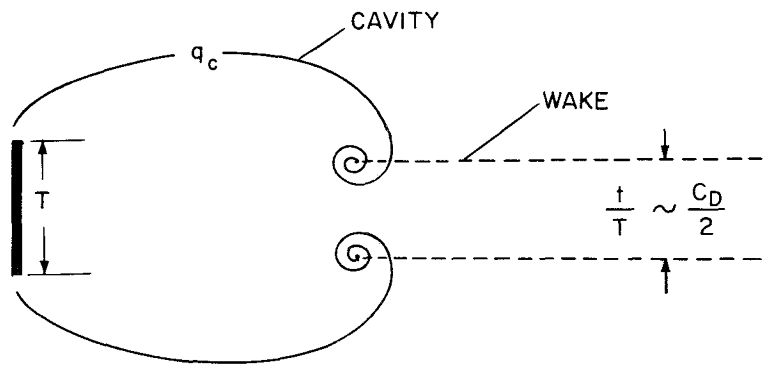

SINGLE SPIRAL VORTEX — SMOOTH WAKE

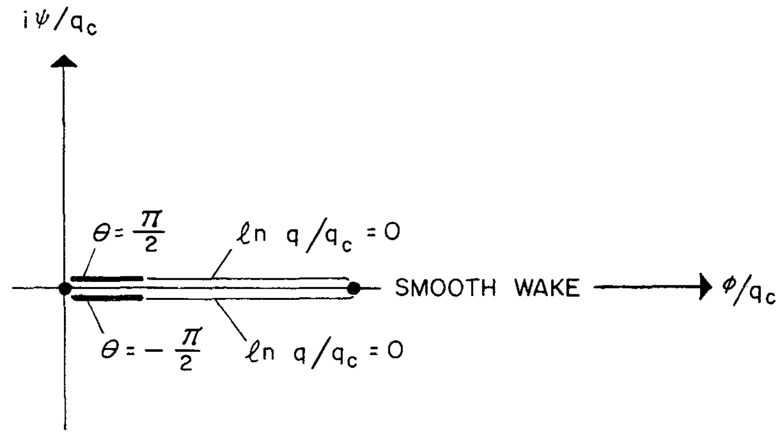

IN BOTH CASES AT INFINITY : $\theta = 0$
AND ASYMPTOTICALLY :

$$\ln q/q_c \sim \ln q_o/q_c + \frac{TC_D}{4\pi}(q_o/q_c)\cdot(\Psi/q_c)^{-1}$$

$$\Psi/q_c = \phi/q_c + i\,\psi/q_c$$

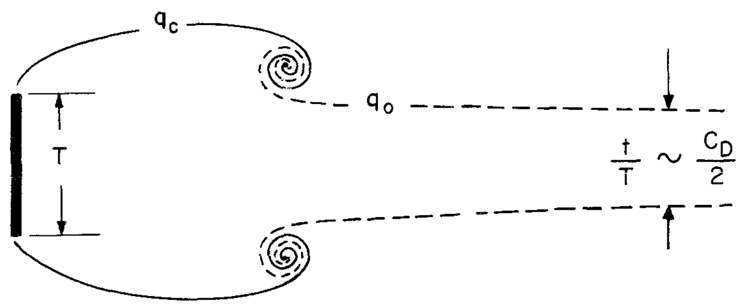

DOUBLE SPIRAL VORTEX – CONSTANT PRESSURE WAKE

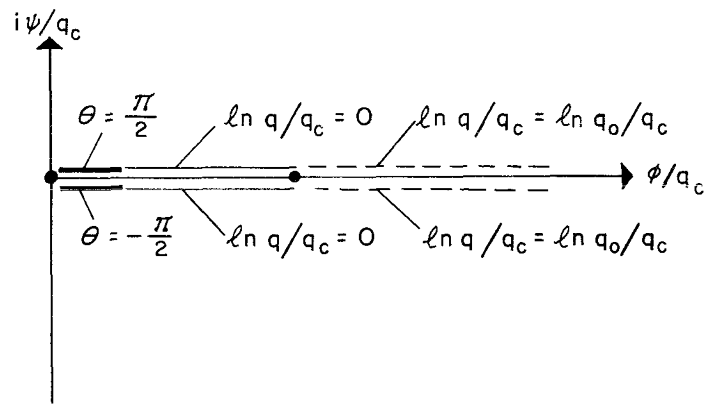

FIGURE 2– SPIRAL VORTEX, TRAILING WAKE MODEL

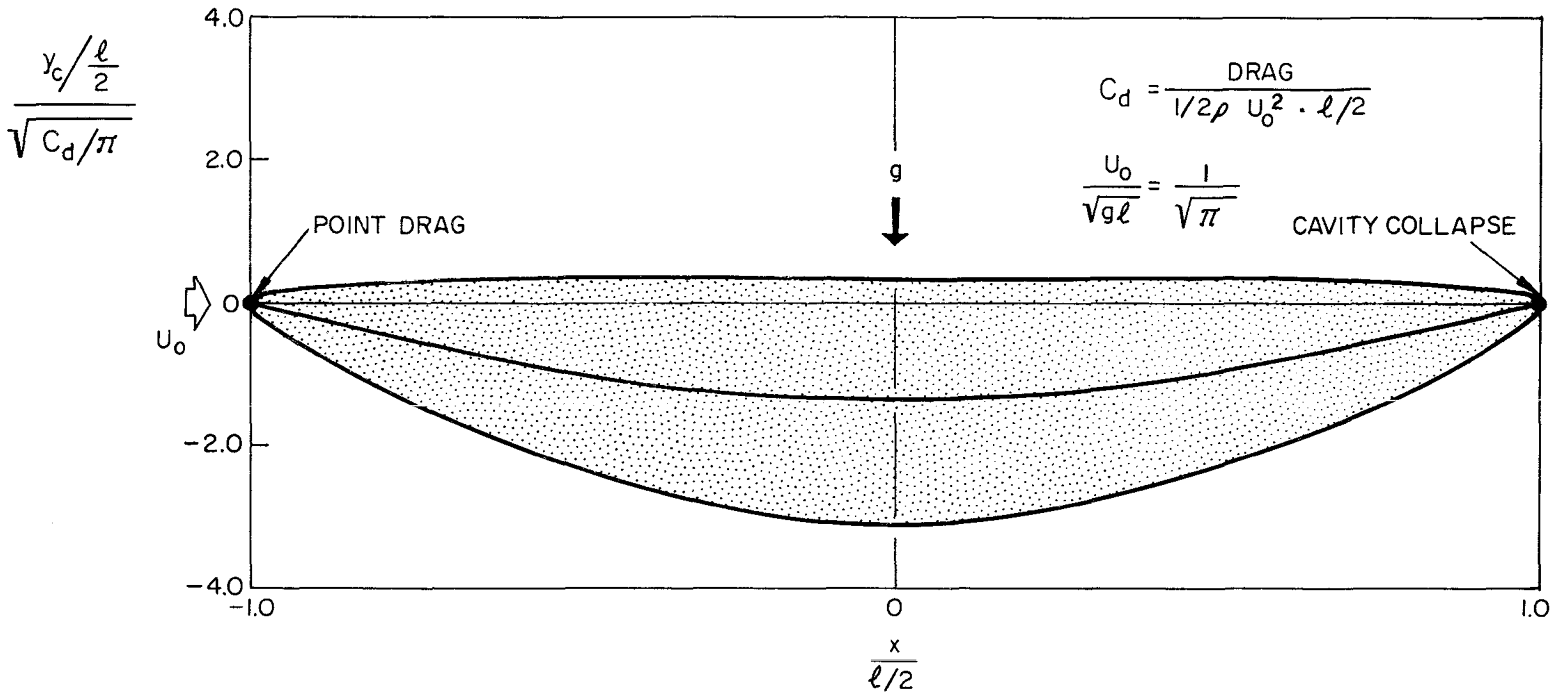

FIGURE 3– THE CAVITY SHAPE IN A TRANSVERSE GRAVITY FIELD ($\sigma = 0$)

UNCLASSIFIED

Security Classification

DOCUMENT CONTROL DATA - R&D (Security classification of title, body of abstract and indexing annotation must be entered when the overall report is classified)		
1. ORIGINATING ACTIVITY (Corporate author) HYDRONAUTICS, Incorporated Pindell School Road, Howard County	2a. REPORT SECURITY CLASSIFICATION Unclassified	
	2b. GROUP	
3. REPORT TITLE THE SHAPE OF CAVITIES IN SUPERCAVITATING FLOWS		
4. DESCRIPTIVE NOTES (Type of report and inclusive dates) Technical Report		
5. AUTHOR(S) (Last name, first name, initial) Tulin, Marshall P.		
6. REPORT DATE April 1965	7a. TOTAL NO. OF PAGES 38	7b. NO. OF REFS 20
8a. CONTRACT OR GRANT NO. Nonr 3435(00)	9a. ORIGINATOR'S REPORT NUMBER(S) Technical Report 121-5	
b. PROJECT NO.		
c.	9b. OTHER REPORT NO(S) (Any other numbers that may be assigned this report)	
d.		
10. AVAILABILITY/LIMITATION NOTICES Qualified requesters may obtain copies of this report from DDC		
11. SUPPLEMENTARY NOTES Presented in Abridged form at the XI International Congress for Theoretical & Applied Mech. Munich-Sept. 1964	12. SPONSORING MILITARY ACTIVITY Office of Naval Research Department of the Navy	

13. ABSTRACT

The shape of cavities in two-dimensional, steady supercavitating flows is discussed. Some new finite cavity models are described; these models feature cavity termination in spiral vortices followed by trailing wakes whose thickness is proportionate to the drag coefficient of the forebody.

Linearized theory, together with point forebodies, is used to derive simple relations between drag, cavitation number and cavity length. The case of a dragless forebody is also considered and the cavity length is shown to depend upon the second moment of the distributed drag.

The influence of both longitudinal and transverse gravity fields on the flow past a body producing drag is discussed. It is shown that in all cases the cavity is caused to be finite. In the case of the transverse field, the cavity is shown to be of a length which corresponds to a Froude number of $(\pi)^{-\frac{1}{2}}$ and it is, rather surprisingly, deflected over its mid-part in the same direction in which gravity acts.

DD FORM 1 JAN 64 1473

UNCLASSIFIED

Security Classification

DISTRIBUTION LIST
(Contract Nonr-3435(00))

Chief of Naval Research Department of the Navy Washington 25, D. C. Attn: Codes 438	3
461	1
463	1
466	1
Commanding Officer Office of Naval Research Branch Office 495 Summer Street Boston 10, Massachusetts	1
Commanding Officer Office of Naval Research Branch Office 207 West 24th Street New York 11, New York	1
Commanding Officer Office of Naval Research Branch Office 1030 East Green Street Pasadena, California	1
Commanding Officer Office of Naval Research Branch Office 1000 Geary Street San Francisco 9, California	1
Commanding Officer Office of Naval Research Branch Office Box 39, Navy No. 100 Fleet Post Office New York, New York	25
Director U. S. Naval Research Laboratory Washington 25, D. C. Attn: Code 2027	6
Chief, Bureau of Naval Weapons Department of the Navy Washington 25, D. C. Attn: Codes RUTO-32	1
RRRE	1
RAAD	1
RAAD-222	1
DIS-42	1
Chief, Bureau of Ships Department of the Navy Washington 25, D. C. Attn: Codes 310	1
312	1
335	1
420	1
421	1
440	1
442	1
449	1
436	2
Chief, Bureau of Yards and Docks Department of the Navy Washington 25, D. C. Attn: Code D-400	1
Commander U. S. Naval Ordnance Test Station China Lake, California Attn: Code 753	1

Commander
Planning Department
U. S. Naval Weapons Laboratory
Dahlgren, Virginia 1

Commander
U. S. Naval Ordnance Laboratory
White Oak, Maryland 1

Dr. A. V. Hershey
Computation and Exterior
Ballistics Laboratory
U. S. Naval Weapons Laboratory
Dahlgren, Virginia 1

Superintendent
U. S. Naval Academy
Annapolis, Maryland
Attn: Library 1

Superintendent
U. S. Naval Postgraduate School
Monterey, California 1

Commandant
U. S. Coast Guard
1300 E. Street, N. W.
Washington, D. C. 1

Secretary Ship Structure
Committee
U. S. Coast Guard Headquarters
1300 E. Street, N. W.
Washington, D. C. 1

Commander
Military Sea Trans. Service
Department of the Navy
Washington 25, D. C. 1

U. S. Maritime Administration
GAO Building
441 G. Street, N. W.
Washington, D. C.
Attn: Div. of Ship Design 1
Div. of Research 1

Superintendent
U. S. Merchant Marine Academy
Kings Point, Long Island,
New York
Attn: CAPT L.S. McCready
(Dept. of Engr.) 1

Commanding Officer and Director
U. S. Navy Mine Defense Lab.
Panama City, Florida 1

Commanding Officer
NROTC and Naval Adm. Unit
Massachusetts Institute of
Technology
Cambridge 39, Massachusetts 1

U. S. Army Transportation
Research and Dev. Command
Fort Eustis, Virginia
Attn: Marine Transport Div. 1

Mr. J. B. Parkinson
National Aeronautics and
Space Administration
1512 H. Street, N. W.
Washington 25, D. C. 1

Director
Langley Research Center
Langley Station
Hampton, Virginia
Attn: Mr. I.E. Garrick 1
Mr. D.J. Marten 1

University of Michigan
Ann Arbor, Michigan
Attn: Professor R.B. Couch
(Dept. of Naval Arch.) 1
Professor W.W. Willmarth
(Aero Engr. Dept.) 1

Dr. L. G. Straub, Director
St. Anthony Falls Hydraulic Lab.
University of Minnesota
Minneapolis 14, Minnesota 1
Attn: Mr. J. N. Wetzel 1
Professor B. Silverman 1

Professor J. J. Foody
Engineering Department
New York State University
Maritime College
Fort Schulyer, New York 1

New York University
Institute of Mathematical
Sciences
25 Waverly Place
New York 3, New York
Attn: Professor J. Keller 1
Professor J. J. Stoker 1

The Johns Hopkins University
Department of Mechanical Engr.
Baltimore 18, Maryland
Attn: Professor S. Corrsin 1
Professor O.M. Phillips 2

Massachusetts Institute of Tech.
Department of Naval Arch.
and Marine Engr.
Cambridge 39, Massachusetts
Attn: Prof. M.A. Abkowitz 1

Dr. G. F. Wislicenus
Ordnance Research Laboratory
Pennsylvania State University
University Park, Pennsylvania 1
Attn: Dr. M. Sevik 1

Professor R. C. DiPrima
Department of Mathematics
Rensselaer Polytechnic Institute
Troy, New York 1

Stevens Institute of Technology
Davidson Laboratory
Castle Point Station
Hoboken, New Jersey
Attn: Mr. D. Savitsky 1
Mr. J. P. Breslin 1
Mr. C. J. Henry 1
Mr. S. Tsakonas 1

Webb Institute of Naval
Architecture
Crescent Beach Road
Glen Cove, New York
Attn: Professor E.V. Lewis 1
Technical Library 1

Director
Woods Hole Oceanographic Inst.
Woods Hole, Massachusetts 1

Executive Director
Air Force Office of Scientific
Research
Washington 25, D. C.
Attn: Mechanics Branch 1

Commander
Wright Air Development Division
Aircraft Laboratory
Wright-Patterson Air Force
Base, Ohio
Attn: Mr. W. Mykytow,
Dynamics Branch 1

Dr. S.F. Hoerner
148 Busteed Drive
Midland Park, New Jersey 1

Boeing Airplane Company
Seattle Division
Seattle, Washington
Attn: Mr. M.J. Turner 1

Electric Boat Division
General Dynamics Corporation
Groton, Connecticut
Attn: Mr. Robert McCandliss 1

General Applied Sciences Lab., Inc.
Merrick and Stewart Avenues
Westbury, L. I. New York 1

Gibbs and Cox, Inc.
21 West Street
New York, New York 1

Grumman Aircraft Engineering Corporation, Bethpage,
Long Island, New York
Attn: Mr. E. Baird 1
Mr. E. Bower 1
Mr. W.P. Carl 1

Lockheed Aircraft Corporation
Missiles and Space Division
Palo Alto, California
Attn: R.W. Kermeen 1

Midwest Research Institute
425 Voker Blvd.
Kansas City 10, Missouri
Attn: Mr. Zeydel 1

Director, Department of Mechanical Sciences
Southwest Research Institute
8500 Culebra Road
San Antonio 6, Texas
Attn: Dr. H.N. Abramson 1
Mr. G. Ransleben 1
Editor, Applied Mechanics Review 1

Convair
A Division of General Dynamics
San Diego, California
Attn: Mr. R.H. Oversmith 1
Mr. H.T. Brooke 1

Hughes Tool Company
Aircraft Division
Culver City, California
Attn: Mr. M.S. Harned 1

HYDRONAUTICS, Incorporated
Pindell School Road
Howard County
Laurel, Maryland
Attn: Mr. Phillip Eisenberg 1

Rand Development Corporation
13600 Deise Avenue
Cleveland 10, Ohio
Attn: Dr. A.S. Iberall 1

U. S. Rubber Company
Research and Development Dept.
Wayne, New Jersey
Attn: L.M. White 1

Technical Research Group, Inc.
Route 110
Melville, New York
Attn: Dr. Jack Kotik 1

Professor J. William Holl
Dept. of Aeronautical Engr.
The Pennsylvania State Univ.
Ordnance Research Laboratory
P. O. Box 30
State College, Pennsylvania 1

Professor Brunelle
Department of Aeronautical
Engr.
Princeton University
Princeton, New Jersey 1

National Academy of Science
National Research Council
Committee on Undersea Warfare
2101 Constitution Avenue
Washington 25, D. C. 1

Dr. Harvey Brooks
School of Applied Science
Harvard University
Cambridge, Massachusetts 1